Quantum superposition of charge states on capacitively coupled superconducting islands

C. P. Heij, D. C. Dixon,* C. H. van der Wal, P. Hadley, and J. E. Mooij
Applied Physics and DIMES, Delft University of Technology, Lorentzweg 1, 2628 CJ Delft, The Netherlands
(Received 17 January 2003; published 18 April 2003)

We investigate the ground state properties of a system containing two superconducting islands coupled capacitively by a wire. The ground state is a macroscopic superposition of charge states, even though the islands cannot exchange charge carriers. The ground state of the system is probed by measuring the switching current of a Bloch transistor containing one of the islands. Calculations based on superpositions of charge states on both islands show good agreement with the experiments. The ability to couple quantum mechanical charge fluctuations in two neighboring devices using a wire is relevant for realizing quantum computation with this kind of circuit.

DOI: 10.1103/PhysRevB.67.144512 PACS number(s): 73.23.Hk, 74.50.+r, 85.25.Hv

Quantum phenomena in artificially fabricated structures has received much attention lately largely due to the interest in performing quantum computation in such systems. If quantum states can be manipulated in an artificially fabricated circuit, there is hope that the circuit could be increased in complexity to a size where it may be able to perform useful functions. Quantum coherence in fabricated structures has been discussed for the charge states in quantum dots[1] and for nuclear spin states of impurity atoms embedded in silicon.[2] Measurements have been performed using charge states on a single superconducting island[3–6] and flux states in a circuit containing a superconducting loop.[7–9] In this paper, we show that the ground state of a system containing two superconducting islands that are capacitively coupled by a wire, can be in a superposition of spatially distinct charge states. This type of coupling is of importance for realizing complex quantum circuits with mesoscopic charge devices.

Figure 1 shows a scanning electron microscope (SEM) photo of the sample and the circuit schematic. The two square superconducting islands labeled L and R play a central role in this circuit. They are spaced 3 μm apart and are coupled by a wire that contains two capacitors in series. There is no exchange of charge carriers between the two superconducting islands; the interaction between the islands is purely electrostatic. Each island can exchange charge with its superconducting leads through small-capacitance Josephson junctions. Together with the leads and the left gate electrode, the island L forms a Bloch transistor that was current biased by an external current source. Single Bloch transistors have been studied in detail and their behavior is well understood.[10–15] The leads of island R are joined in a small loop, transforming the island into a Cooper-pair box with tunable Josephson energy, one of the promising candidates for the realization of a charge qubit.[3,16]

The state of this circuit can be conveniently described by the charge states of the two islands $|n_L,n_R\rangle$. Here n_L is the number of excess Cooper pairs on the left island and n_R is the number of excess Cooper pairs on the right island. For certain values of the gate voltages and the applied flux, the ground state is very similar to the superposition state $(|0,1\rangle + |1,0\rangle)/\sqrt{2}$. In this state, the electric field in the capacitances between the two islands is in a superposition of two values. Since there is no tunneling of Cooper pairs between the left and right island, this superposition of charge states cannot be viewed as a single Cooper pair with some probability of being found on the left island and some probability of being found on the right island. Alternatively, the experiment *can* be explained by describing the whole circuit with a single collective ground state where the charge and the electric field are in a superposition throughout a region about 3 μm in size. A comparison of the measurements and a model that describes this circuit as a single quantum system is given below. Note that our experiment probes the ground state of the circuit: the effective temperature of the system is very low, and the control of the circuit (bias current, gate voltages, and magnetic flux) is performed at time scales much slower than what is required for adiabatic control of the system. Under these conditions, we still find that a change of the flux bias of the box (R) changes the readout of the Bloch transistor (L), even though the coupling by the wire is purely electrostatic. This phenomena is the due to the fact that wire couples the quantum fluctuations in the charges of the islands L and R, and is used to prove that the ground state of the system is for certain control parameters nominally equal to $(|0,1\rangle + |1,0\rangle)/\sqrt{2}$.

The device was fabricated on a thermally oxidized silicon substrate using a high-resolution electron-beam pattern generator at 100 kV. Each layer of the circuit was defined using a double-layer resist and was aligned to prefabricated Pt markers. The bottom layer of the circuit consisted of a 25 nm thick aluminum film that was patterned to form the lower electrodes of the coupling capacitors and a shunt capacitor C_S. The aluminum was then oxidized by heating it to 200 °C in an O_2 plasma at 100 mTorr for 5 min. The resulting Al_xO_y formed an 8 nm thick dielectric layer for the capacitors. The insulating properties of this oxide were tested by fabricating a 1×1 mm^2 $Al/Al_xO_y/Al$ overlap capacitor which showed no leakage ($R>10$ GΩ) for voltages up 3 V. The islands deposited in the second aluminum layer form the top electrodes of the capacitors. The coupling capacitors can be seen in the SEM photo where the two square islands overlap the dumbbell-shaped structure in the middle of the photo. The effective capacitance C_m of the two coupling capacitors in series was 2 fF. The 120 pF shunt capacitor C_S parallel to the Bloch transistor and a 5 pF gate capacitor connected to the loop were similarly defined but are not visible in the SEM

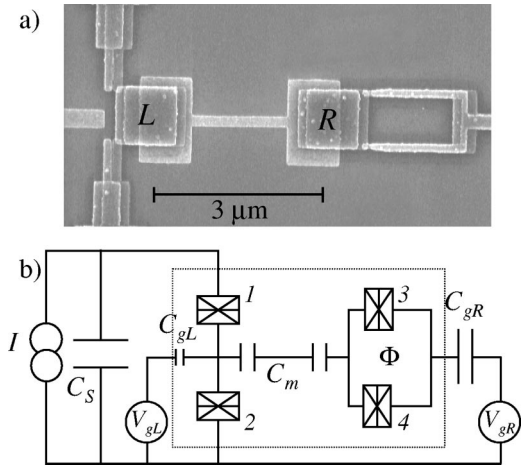

FIG. 1. (a) A scanning electron microscope photograph of the device shows the Bloch transistor on the left and on the right the Cooper pair box in the form of a superconducting loop. (b) The schematic circuit diagram shows how the sample was embedded in the circuit. The dotted line in the diagram indicates the part of the circuit that can be seen in the SEM photo.

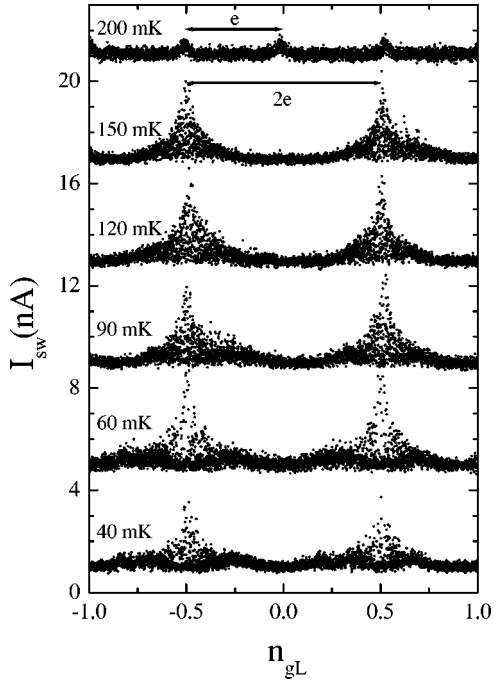

FIG. 2. Switching-current results (dots) versus n_{gL} for different temperatures, $n_{gR}=1/2$ and $\Phi=0$. The curves are offset 4 nA for clarity. The odd-even transition temperature was 190 mK, while the main peaks partly collapse below ~80 mK due to poisoning effects (see text).

photo. The shunt capacitor C_S protects the device against electrostatic discharge and suppresses voltage fluctuations across the transistor that degrade low-noise electronic control of the transistor. The tunnel junctions were formed by shadow evaporation. All the junctions were defined to be equal. The series resistance of the two junctions in the transistor was 18 kΩ. From the current-voltage characteristics and the size observed in the SEM photos, the junction capacitances were estimated to be $C=1$ fF. The area of the loop was 1.7 μm^2, giving rise to a magnetic field periodicity of 1.2 mT. The product of the inductance of the loop times the critical current of the junctions is much less than a flux quantum $LI_c \ll \Phi_0$ so that quantum fluctuations of the flux in the loop were very small and could be neglected. Furthermore, $C_{gL}=40$ aF and the effective gate capacitance C_{gR} to island R was 2 fF; the effective gate capacitance is the series capacitance of the two Josephson junctions and the 5 pF gate capacitor [on the right in Fig. 1(b)]. In the remainder of this paper the settings of the gate voltages V_{gL} and V_{gR} will be represented by dimensionless induced gate charges $n_{gL}=C_{gL}V_{gL}/2e$ and $n_{gR}=C_{gR}V_{gR}/2e$. These definitions assume that the influence of background charges have already been compensated for by an offset in V_{gL} and V_{gR}.[17]

The sample was mounted in a microwave-tight copper box connected to the mixing chamber of a dilution refrigerator with a base temperature of 5 mK. All of the measurement leads were filtered using rfi-feedthrough filters at room temperature and copper-powder low-pass filters at the mixing chamber. The current through the sample was ramped with a rate of 1.6×10^{-5} A/s. The voltage over the sample was measured in a four-probe configuration using dedicated electronics.

The current-voltage characteristics of the Bloch transistor SET show a supercurrent branch around zero voltage. When the Bloch transistor was current biased, the system remained on the supercurrent branch until a certain bias current was exceeded. There was then a discontinuous jump in the voltage from nearly zero voltage on the supercurrent branch to a voltage of about $2\Delta/e$, where Δ is the superconducting gap of aluminum, 200 μeV for our thin-layered aluminum. The switching current was defined as the current where the voltage over the sample exceeded 1 μV. A sample-and-hold circuit read out the switching current at a rate of 20 Hz.

Figure 2 shows measurements of the switching current I_{SW} versus the gate charge n_{gL} that is induced on island L of the Bloch transistor for various temperatures. The black dots represent single switching-current events. Above 190 mK the switching current showed a weak modulation that was e periodic in the induced charge. Upon lowering the temperature below 190 mK, the switching current became $2e$ periodic in the induced charge. This transition temperature is in agreement with the critical odd-even temperature.[11] Even though the data is clearly $2e$ periodic below 190 mK, some so-called poisoning effects remain. At values of $n_{gL}=0.5$ mod 1, the Coulomb blockade for Cooper pair transport is minimized and the switching-current modulations show maximums (in agreement with theory[10,14]). However, at these n_{gL} values the distribution of the switching currents becomes very broad. We attribute this to the fact that at $n_{gL}=0.5$ mod 1 the Bloch transistor is most sensitive to quasiparticle poisoning:[10,14] The effect that the switching current is suppressed by the presence of an unpaired electron on the island. The broad switching-current distribution indicates that the typical time scale for an unpaired electron to enter or leave the island is comparable to the switching-current measurements time. Moreover, we observed that the poisoning got worse when

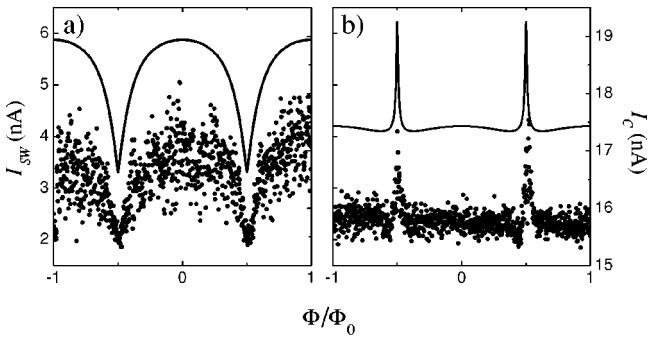

FIG. 3. The measured switching current (dots) and the calculated critical current (solid lines) are plotted as a function of the magnetic flux for two gate configurations. The scale for the switching-current measurements is on the left, the scale for the critical current calculations is on the right. The gates were tuned to (a) $n_{gL}=1/2$, $n_{gR}=1/2$, and (b) $n_{gL}=0.75$, $n_{gR}=0.44$. The temperature of this measurement was 110 mK.

lowering the temperature. This is not in agreement with the model presented in Refs. 10,14. Very similar observations of this unusual long-time-scale poisoning were reported and studied in more detail in Refs. 18,17, but are not fully understood. We performed our experiments at 110 mK where the poisoning effects were minimal. Also, note that the effect of poisoning only shows up as an increased distribution of switching-current values below maximums in the switching current. The poisoning effects do therefore not obscure a study of the maximums in the $2e$-periodic switching-current modulation.

The measurements in Fig. 3 show that the switching current of the Bloch transistor (L) depends on the magnetic flux threading the loop of the box (R). This is observed, even though the two devices have a purely electrostatic interaction, and have their gate charges fixed in these measurements. The modulation of the switching current is periodic in the applied flux with a periodicity of Φ_0. The behavior depends nontrivially on the combination of normalized gate charges n_{gL} and n_{gR}. There are sharp dips in the switching current as a function of flux for induced charges $n_{gL}=1/2$, $n_{gR}=1/2$ [Fig. 3(a)] while sharp peaks appear in the switching-current behavior for induced charges $n_{gL}=0.75$, $n_{gR}=0.44$ [Fig. 3(b)]. The dependence of the switching current on the gate voltages and flux through the loop agrees well with the dependence of the critical current attained from calculations, shown as solid lines. The calculations are based on a model that describes the circuit in terms of a single quantum mechanical wave function.

The model used to describe this system was arrived at by quantizing the macroscopic current conservation equations for the circuit shown in Fig. 1. In general, the dynamics of circuit can be described in terms of the four gauge invariant phases γ_i, of the junctions. However, there are two restrictions on the four phases. The fluxoid quantization condition relates the phases of junctions in the loop to the externally applied flux Φ, $\gamma_3+\gamma_4=2\pi\Phi/\Phi_0$, where $\Phi_0=h/2e$ is the superconducting flux quantum. As long as there is no voltage across the Bloch transistor, the phases of the two junctions of the Bloch transistor are related to a time-independent external phase θ, $\gamma_1+\gamma_2=\theta$, which can be considered a classical variable.[15] With these two restrictions on the four junction phases, two independent variables can be defined. We take these variables to be $\phi_L=(\gamma_1-\gamma_2)/2$ and $\phi_R=(\gamma_3-\gamma_4)/2$. We assume that all the junctions have identical capacitances and critical currents ($C=C_i$, $I_c=I_{ci}$). When expressed in the charge basis, the Hamiltonian that follows from this analysis is

$$
\begin{aligned}
H=\sum_{n_L,n_R}\Bigg\{ & [E_C(n_L-n_{gL})^2+E_C(n_R-n_{gR})^2 \\
& +E_m(n_L-n_{gL})(n_R-n_{gR})]|n_L,n_R\rangle\langle n_L,n_R| \\
& -\frac{E_J}{2}\cos\left(\frac{\theta}{2}\right)(|n_L,n_R\rangle\langle n_L-1,n_R|+|n_L+1,n_R\rangle\langle n_L,n_R|) \\
& -\frac{E_J}{2}\cos\left(\frac{\pi\Phi}{\Phi_0}\right)(|n_L,n_R\rangle\langle n_L,n_R-1| \\
& +|n_L,n_R+1\rangle\langle n_L,n_R|)\Bigg\}, \qquad (1)
\end{aligned}
$$

where n_L and n_R are the number of excess Cooper pairs on the left and the right island, C_Σ is the sum of all capacitors connected to an island, $E_C=e^2C_\Sigma/[2(C_\Sigma^2-C_m^2)]$ is the charging energy, $E_m=e^2C_m/(C_\Sigma^2-C_m^2)$ is the electrostatic interaction energy, and $E_J=\hbar I_c/2e$ is the Josephson coupling energy. For this circuit $C_\Sigma=3f$F, $E_C=E_m=27$ μeV and $E_J=70$ μeV. To determine the ground state, we diagonalized the Hamiltonian matrix (1) and selected the lowest eigenvalue and corresponding eigenvector. The matrix was truncated, such that it was spanned by the 25 charge states $|n_L,n_R\rangle$ with the lowest charging energies. We checked that taking more charge states into account did not change our numerical results: The ground state has negligible probability amplitudes for charge states $|n_L,n_R\rangle$ with high charging energies.

Once the ground state $|\Psi_0\rangle$ was determined, the expectation value of the Josephson supercurrent flowing through the Bloch transistor was evaluated using the expression

$$\langle I_s(\theta)\rangle=\left\langle\Psi_0\left|\frac{2e}{\hbar}\frac{dH}{d\theta}\right|\Psi_0\right\rangle. \qquad (2)$$

The maximum supercurrent, or critical current, is $I_C=\max I_s(\theta)$. Calculations of I_C are shown as solid lines in Fig. 3. For other combinations of gate charges, there is also good qualitative agreement between the model and the experiments. The quantitative difference between the theory and the experiment is due to the dissipative environment that has not been included in this model. Joyez *et al.* have shown that the low-impedance environment of the Bloch transistor reduces the measured switching current below the critical current that is calculated with this simple theory.[14] The differences between the calculated critical current and the measured switching current with the specified junction resistances are similar to values reported by Flees *et al.*[12]

The flux threading the loop changes the effective Josephson energy of the Cooper pair box and hence the ratio E_J/E_C. The expectation value of the charge on island R strongly depends on this ratio. Consequently, changing the flux also changes the expectation value of the charge on island R. Part of this charge is induced on island L via the mutual capacitance C_m. Thus one can expect a modulation of the switching current of the transistor (L) when changing the flux in the loop of the box (R). However, this does not hold at a gate charge of $n_{gR}=1/2$. At this gate charge, the expectation value of the charge on the island is always e, independent of the ratio E_J/E_C.[16] The measurements of Fig. 3(a) were taken at gate charge $n_{gR}=1/2$, but still show a modulation of the switching current. Consequently the data cannot be explained by simply assuming that a flux-induced shift of the average charge on island R modulates the switching current of the Bloch transistor.

The fact that the flux applied to the loop of the box (R) nevertheless does modulate the switching current of the transistor (L) in Fig. 3(a) can be qualitatively understood with the following argument, assuming a collective ground state for the whole system (as in the model above). When both gates of our system are tuned to half a Cooper pair, the states $|0,1\rangle$ and $|1,0\rangle$ have the lowest electrostatic energy. When the effective Josephson energy of the box (R) is small ($\Phi=\Phi_0/2$) compared to its charging energy, the ground state will be close to $(|0,1\rangle+|1,0\rangle)/\sqrt{2}$, resulting in relatively small charge fluctuations on both islands. When the effective Josephson energy of the box (R) increases and becomes larger than its charging energy (reaching a maximum for $\Phi=0$), the stronger Josephson coupling will coherently mix other charge states such as $|0,0\rangle$ and $|1,1\rangle$ in the ground state. This not only enhances the charge fluctuations in island R, but also the fluctuations of island L, and thereby the critical current of the transistor. The flux-modulated switching current for $n_{gL}=1/2$ and $n_{gR}=1/2$ provides therefore evidence for our assumption that the two circuits are in a collective ground state, and the interpretation that the two coupled charge devices exchange quantum fluctuations via the wire. The charge fluctuations are strongly coupled through capacitor C_m, and when sweeping the flux from 0 to $\Phi_0/2$, the charge fluctuations will be minimal at $\Phi_0/2$, resulting in a minimal switching current, as confirmed in Fig. 3(a).

Figure 4 shows measurements of the switching current $I_{\rm sw}$ and calculations of I_C as a function of the induced charges on the islands at an enclosed magnetic flux of 0 and $\Phi_0/2$. The data presented is the highest switching current out of 20 repeated measurements. This is to exclude effects of poisoning. Because of the gate cross capacitances, it was necessary to tune both gates simultaneously to sweep orthogonally through induced charge space. Figure 4(a) shows that the switching current is $2e$ periodic in both n_{gL} and n_{gR}, confirming that quasiparticle poisoning is absent on both islands. When $\Phi=0$, both $I_{\rm sw}$ and I_C are almost independent of n_{gR}.

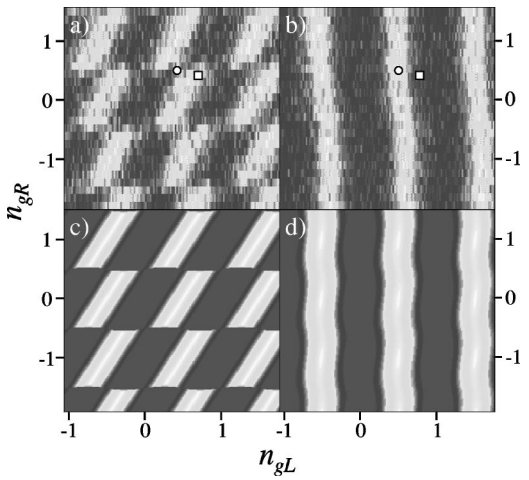

FIG. 4. The maximum measured switching current [(a),(b)] and the calculated maximum supercurrent [(c),(d)] are plotted as a function of the charge induced on the two gates for $\Phi=\Phi_0/2$ [(b,d)] and [(a,c)]. Dark (light) is low (high) switching current. The experimental data presents the highest switching current out of 20 repetitions to be robust against poisoning effects (see text). The symbols denote the gate voltages where where the data of Fig. 3(a) (○) and Fig. 3(b) (□) was extracted. The temperature of this measurement was 110 mK.

An intuitive explanation is that for $\Phi=0$ the effective Josephson energy $E_J\cos(\pi\Phi/\Phi_0)=70\ \mu$eV is larger than the charging energy $E_C=27\ \mu$eV on island R. Cooper pairs are not localized on island R and the circuit behaves as a single Bloch transistor with a capacitance to ground formed by C_m and $2C$ in series. The remaining small wiggles in the calculation indicate that some charging effects should still remain, but they are outside the resolution of our switching-current measurements. When $\Phi=\Phi_0/2$, E_J is very small and Cooper pairs are localized on the island R. The saw-tooth-like dependence of $I_{\rm sw}$ on n_{gR} indicates the dominance of charging effects on island R. The dots indicate the gate voltages where the data shown in Figs. 3(a) and 3(b) was extracted. These are the points where the flux modulation is most pronounced.

In conclusion, all switching-current measurements have the same gate voltage and flux dependence as a model in which we calculate the maximum supercurrent of the ground state of the combined system. The ground state is a superposition of spatially distinct charge states, where the coupling capacitor not only couples charge but also strongly correlates the quantum mechanical charge fluctuations on both islands. The good agreement between this model and the experiment implies that it was possible to prepare the circuit in a superposition of charge states. A macroscopic superposition of this sort is necessary to achieve the entanglement used in a controlled-NOT gate in quantum computation. In principle it should also be possible to measure entanglement in such systems of coupled superconducting islands.

*Present address: Physics Department, Wehr Physics Building, Marquette University, Milwaukee, WI 53233.
[1] T. H. Oosterkamp, T. Fujisawa, W. G. van der Wiel, K. Ishibashi, R. V. Hijman, S. Tarucha, and L. P. Kouwenhoven, Nature (London) **395**, 873 (1998).
[2] B. E. Kane, Nature (London) **393**, 133 (1998).
[3] Yu. Makhlin, G. Schön, and A. Schnirman, Nature (London) **398**, 305 (1999).
[4] Y. Nakamura, Yu. A. Pashkin, and J. S. Tsai, Nature (London) **398**, 786 (1999).
[5] Y. Nakamura, Yu. A. Pashkin, T. Yamamoto, and J. S. Tsai, Phys. Rev. Lett. **88**, 047901 (2002).
[6] D. Vion, A. Aassime, A. Cottet, P. Joyez, H. Pothier, C. Urbina, D. Esteve, and M. H. Devoret, Science **296**, 886 (2002).
[7] J. E. Mooij, T. P. Orlando, L. Levitov, Lin Tian, Caspar H. van der Wal, and Seth Lloyd, Science **285**, 1036 (1999).
[8] J. R. Friedman, V. Patel, W. Chen, S. K. Tolpygo, and J. E. Lukens, Nature (London) **406**, 43 (2000).
[9] C. H. van der Wal, A. C. J. ter Haar, F. K. Wilhelm, R. N. Schouten, C. J. P. M. Harmans, T. P. Orlando, Seth Lloyd, and J. E. Mooij, Science **290**, 773 (2000).
[10] K. A. Matveev, M. Gisselfält, L. I. Glazman, M. Jonson, and R. I. Shekhter, Phys. Rev. Lett. **70**, 2940 (1993).
[11] M. T. Tuominen, J. M. Hergenrother, T. S. Tighe, and M. Tinkham, Phys. Rev. Lett. **69**, 1997 (1992).
[12] D. J. Flees, S. Han, and J. E. Lukens, Phys. Rev. Lett. **78**, 4817 (1997).
[13] M. Matters, W. J. Elion, and J. E. Mooij, Phys. Rev. Lett. **75**, 721 (1995).
[14] P. Joyez, P. Lafarge, A. Filipe, D. Esteve, and M. H. Devoret, Phys. Rev. Lett. **72**, 2458 (1994).
[15] P. Joyez, Ph.D. thesis, Université Paris 6, 1995.
[16] V. Bouchiat, D. Vion, P. Joyez, D. Esteve, and M. H. Devoret, Phys. Scr. **T76**, 165 (1998); J. Supercond. **12**, 789 (1999).
[17] C. H. van der Wal and J. E. Mooij, J. Supercond. **12**, 807 (1999).
[18] V. Bouchiat, Ph.D. thesis, Université Paris 6, 1997.